

# Formation of Plasmid-Based Transfection Complexes with an Acid-Labile Cationic Lipid: Characterization of *in Vitro* and *in Vivo* Gene Transfer

Jeremy A. Boomer,<sup>1</sup> David H. Thompson,<sup>1,4</sup> and Sean M. Sullivan<sup>2,3</sup>

Received January 7, 2002; accepted May 22, 2002

**Purpose.** This study tests the hypothesis that gene transfer efficiency may be improved through the use of transiently stable transfection complexes that degrade within endosomal compartments and promote plasmid escape into the cytosol.

**Method.** An acid labile cationic lipid, *O*-(2R-1,2-di-*O*-(1'Z, 9'Z-octadecadienyl)-glycerol)-3-*N*-(bis-2-aminoethyl)-carbamate (BCAT), was designed, synthesized, and tested for enhanced gene transfer activity relative to non-labile controls.

**Results.** The *O*-alkenyl chains of BCAT were completely hydrolyzed after 4 h incubation in pH 4.5 buffer at 25°C. Addition of BCAT to plasmid DNA in 40% ethanol followed by ethanol evaporation yielded transfection complexes that transfected several cell types in the presence of fetal calf serum and without the need of a helper lipid. Transfection complexes prepared from BCAT displayed higher luciferase expression than the corresponding DCAT complexes (an acid-insensitive derivative of BCAT) for all cell types tested. Uptake studies showed that this increase was not due to a difference in the amount of DNA being delivered. FACS analysis for GFP expression showed that BCAT transfection complexes yielded 1.6 more transfected cells and 20% higher log mean fluorescence than DCAT transfection complexes. *In vivo* gene transfer was demonstrated in subcutaneous tumor-bearing mice by systemic administration of a 60 µg plasmid dose. Expression was observed in the lungs and in the tumor, with the highest activity being observed in the lungs.

**Conclusions.** Our results show that increased transfection can be

obtained by coupling the cationic headgroup to the hydrophobic amphiphilic tails via acid-labile bonds. Acid-catalyzed release of the alkyl chains should facilitate dissociation of the cationic lipid headgroup from the plasmid, thus accelerating one of the rate-limiting steps in cationic lipid mediated transfection.

**KEY WORDS:** gene transfer; acid-sensitive lipid; transfection; vinyl ether hydrolysis; endosomal escape; cytoplasmic delivery

## INTRODUCTION

Nonviral gene therapy (1–4) has been applied to the treatment of cancer, cardiovascular disease, and the development of vaccines against infectious pathogens. (Concerns with immunogenicity, toxicity, and viral gene integration, along with a limited loading capacity, surround the use of viral vectors in human gene therapy, despite their demonstrated success.) Most often, the therapeutic gene to be delivered is encoded within plasmid DNA that has been propagated and isolated from bacteria. The plasmid can be administered by itself (i.e., free DNA) or formulated with a variety of cationic synthetic gene delivery vehicles. The vehicles may be comprised of simple polyamines (5,6); bulk polymers (7–9); block copolymers such as PEG-co-PEI (10–12); polypeptides (including poly-L-lysine) (13,14); protamine sulfate (15,16); peptide nucleic acids (17); loligomers (18), polyamidoamine dendrimers (19,20); or cationic liposomes (2,21–23). Initial attempts to improve transfection efficiencies with cationic liposomes have employed headgroup and hydrophobic region modifications as a means for improving lipoplex formation, stability, and efficacy. Although this strategy has led to an extensive library of cationic lipids that have produced modest increases in transfection efficiency, an improved knowledge of cationic lipid structure-activity relationships has evolved from these studies. For example, increasing the amine content (24–26) or increasing the alkyl region fluidity (27) generally leads to increased transfection. Manipulation of the formulation parameters by incorporation of targeting agents or neutral, fusogenic lipids (e.g., DOPE or cholesterol) also leads to modest improvements in transfection (28), although efficiencies are still lower than for viral based vectors. Cationic liposome carriers are typically formulated from a cationic lipid, such as DOTMA, DOTAP, DMRIE, DOGS, and a helper lipid like DOPE. Mixing of cationic liposomes with plasmid DNA yields a transfection complex with a large and variable loading capacity. These complexes are believed to enter the cell by endocytosis, where subsequent expression of the transgene requires the plasmid to escape from the endosomal compartment and be transported into the nucleus for transcription. Each step in this sequence represents a potential cellular or molecular barrier for attaining efficient transfection. Zabler and coworkers (29) identified endosomal escape and disassembly as the most formidable obstacles to efficient gene delivery. These issues are difficult to address because the mechanisms responsible for controlling endosomal escape are unknown and the molecular determinants required to effect plasmid release and nuclear translocation are equally unclear. Thus, inefficient transgene expression in most cases is likely due to suboptimal complex design.

In some cases these problems have been partially mitigated by the development of vehicles that utilize enzymatic cleavage (30,31), disulfide cleavage (32–34), ester cleavage

<sup>1</sup> Department of Chemistry, Purdue University, West Lafayette, Indiana 47907-1393.

<sup>2</sup> Valentis Inc., The Woodlands, Texas.

<sup>3</sup> Current address: Department of Pharmaceutics, College of Pharmacy, University of Florida, Gainesville, Florida.

<sup>4</sup> To whom correspondence should be addressed. (e-mail: davethom@chem.purdue.edu)

**ABBREVIATIONS:** BCAT, *O*-(2R-1,2-Di-*O*-(1'Z, 9'Z-octadecadienyl)-glycerol)-3-*N*-(bis-2-aminoethyl)-carbamate; BCAT-acetal, *O*-(4R-2-(8'Z-Heptadecenyl)-4-hydroxymethyl-1,3-dioxolane)-3-*N*-(bis-2-aminoethyl)-carbamate; CAT, Chloramphenicol acetyltransferase; DCAT, *O*-(1,2-Di-*O*-(9'Z-octadecenyl)-glycerol)-3-*N*-(bis-2-aminoethyl)-carbamate; DOTMA, Chol 4:1N-(1-(2,3-Dioleoyloxy)propyl)-*N,N,N*-trimethylammonium chloride:cholesterol; DPC, 2,2'-Dipyridyl carbonate; FACS, Fluorescence-assisted cell sorting; GCAT, *O*-(1-Glycerol)-3-*N*-(bis-2-aminoethyl)-carbamate; GFP, Green fluorescent protein; HUVEC, Human umbilical vein endothelial cells; Lyso-BCAT, *O*-(2R-1-*O*-(1'Z, 9'Z-Octadecadienylglycerol))-*N*-(bis-2-aminoethyl)-carbamate; NIH-3T3, Mouse fibroblast cells; PBS, Phosphate buffered saline; PEI, Polyethyleneimine; RENCA, Renal carcinoma cells; SCCVII, Squamous carcinoma cells.

(35,36), and pH induced phase transition (37) to destabilize the complex and facilitate endosomal escape. Based on our prior work with diplasmenylcholine as a vehicle that promotes cytoplasmic delivery of liposomal contents from acidic endosomes (38,39), we designed an acid-labile, cationic variant of diplasmenylcholine for use as a transfection agent. We now report on *O*-(2*R*-1,2-di-*O*-(1'*Z*,9'*Z*-octadecadienyl)-glycerol)-*N*-(bis-2-aminoethyl)-carbamate (**BCAT**, Fig. 1), a cationic analog of diplasmenylcholine that utilizes a similar glyceryl bisvinyl ether backbone to effect acid-catalyzed phase transitions. We hypothesized that acid-catalyzed hydrolysis of the vinyl ether linkages in this cationic lipid would facilitate both endosomal escape via destabilization of the endosomal membrane and disassembly by increasing the exchangeability of the cationic head group. *O*-(1,2-Di-*O*-(9'*Z*-octadecyl)-glycerol)-*N*-(bis-2-aminoethyl)-carbamate (**DCAT**), a saturated diether analog of **BCAT**, was also synthesized as a control to test this hypothesis. In the present study we describe the structure, degradation, and transfection properties (*in vitro* and *in vivo*) of **BCAT** and **DCAT** complexes relative to an optimized formulation of DOTMA:Chol.

## RESULTS

### Synthesis of **BCAT** and **DCAT**

The diethylenetriamine cationic headgroup for both **BCAT** and the acid-insensitive control compound, **DCAT**, were coupled with their corresponding dialkyl glyceryl ether anchors as shown in Fig. 1. Mixed carbonates were generated by condensation of the alcohol precursors, (2*R*)-1,2-di-*O*-(1'*Z*, 9'*Z*-octadecadienyl)-glycerol (**1**) and 1,2-di-*O*-(9'*Z*-

octadecanyl)-glycerol (**2**), with dipyrindyl carbonate (DPC) in the presence of triethylamine for 2–4 days. Subsequent addition of 1,5-diphthalamidyl-diethylenetriamine yielded the protected carbamates (**3**, **4**) in 69% yield after chromatography. These intermediates were then deprotected with hydrazine hydrate to give **BCAT** and **DCAT** in 20% overall yield starting from *O*-(*t*-butyldiphenylsilyl)-*sn*-glycerol (40). Thin layer chromatography (TLC), mass spectrometry (MS), and  $^1\text{H}/^{13}\text{C}$  nuclear magnetic resonance (NMR) values confirmed the structure and purity of **BCAT** and **DCAT**.

### Hydrolysis of **BCAT**

**BCAT** hydrolysis was measured under acidic conditions at 25°C using  $^1\text{H}$  NMR and at 37°C using reversed phase high-performance liquid chromatography (RP-HPLC). The expected hydrolysis pathway is shown in Fig. 2A assuming that protonation of the vinyl ether  $\beta$ -carbon is the rate-determining step as reported by Kresge and coworkers for a wide variety of vinyl ether substrates (41). Addition of water to the intermediate carbocation generates a hemiacetal that decomposes to generate one equivalent of fatty aldehyde and a single chain cationic lipid fragment (lyso-**BCAT**) that exists in two isomeric forms depending on whether the cleavage reaction is initiated at the *sn*-1 or *sn*-2 vinyl ether bonds. Regardless of the lyso-**BCAT** intermediate formed in the first step, hydrolysis of the second chain could either proceed in the same fashion (i.e., generating a second equivalent of aldehyde) or the protonated lyso-**BCAT** carbocation intermediate could be intramolecularly trapped by the proximal glycerol hydroxyl, thereby generating a cyclic acetal species (**BCAT**-acetal). This acetal would also be prone to acid-

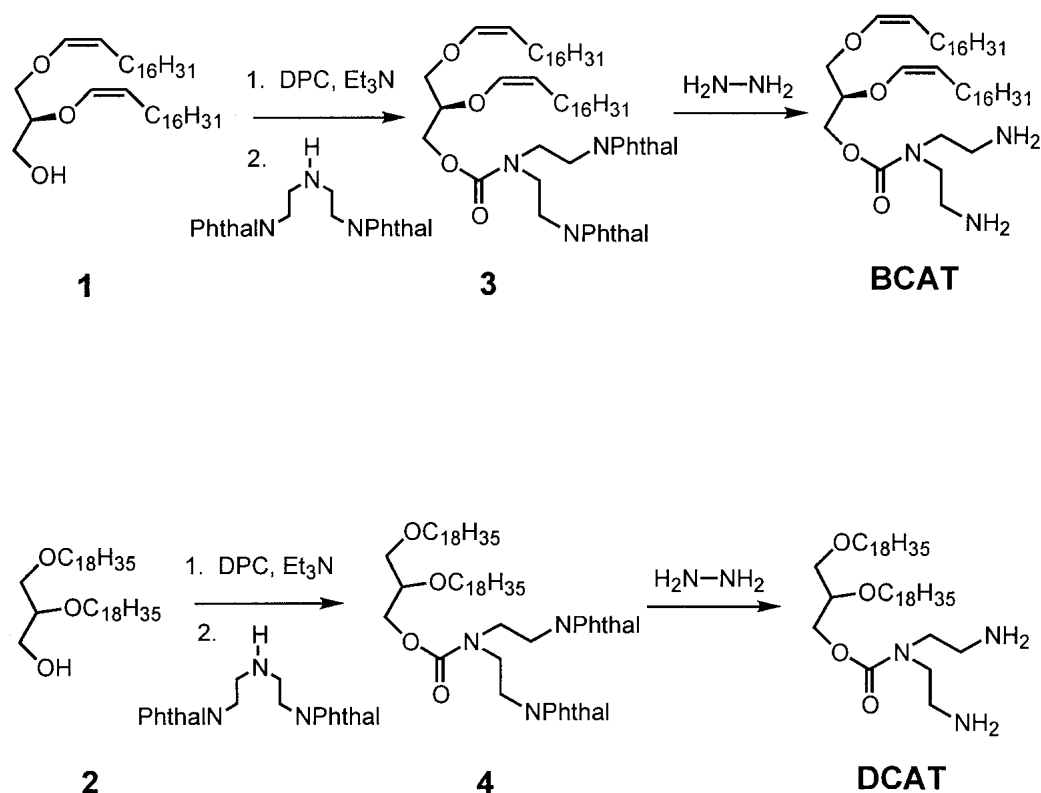


**Fig. 1.** Synthesis of **BCAT** and **DCAT** from their dialkenylglycerol or dialkylglycerol precursors, respectively.

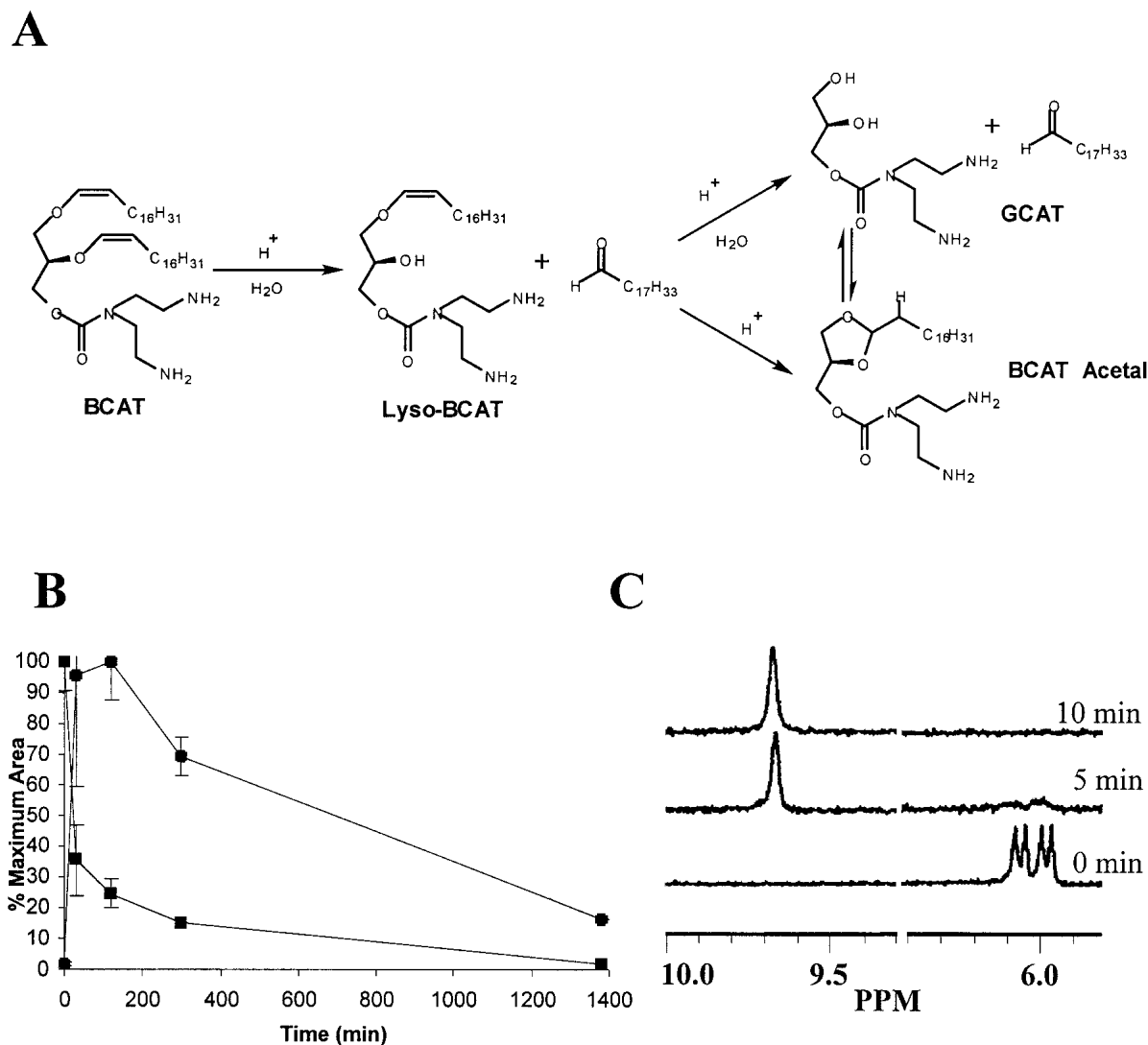


**Fig. 2.** Acid catalyzed hydrolysis of BCAT. (A) Proposed hydrolysis pathway for BCAT. Cleavage of one vinyl ether chain yields lyso-BCAT plus one equivalent of aldehyde. Cleavage of the second chain yields an additional equivalent of aldehyde and GCAT. BCAT-acetal may be produced via a competing intramolecular trapping side reaction or may accumulate via equilibration with GCAT. (B) Time-dependent BCAT hydrolysis at pH 1.0 followed via HPLC: ■ BCAT disappearance kinetics. ● Lyso BCAT formation and disappearance kinetics. (C) Time-dependent  $^1\text{H-NMR}$  spectra of BCAT hydrolysis reaction (90%  $\text{CD}_3\text{CN}$ : 10%  $\text{D}_2\text{O}$  (0.2 M DCl)) monitored at the vinyl ether  $\alpha$  proton (6.05 ppm) and the aldehyde proton (9.68 ppm) resonances.

catalyzed hydrolysis, albeit at rates that are typically much slower than for vinyl ethers.

The rates of BCAT hydrolysis determined by RP-HPLC are shown in Fig. 2B. The peak corresponding to BCAT decreased very rapidly under the acidic reaction conditions (pH 1.0), losing 80% of its initial area within 200 min (less than 3% remained after 24 h). This rapid decrease in the BCAT concentration correlated with the rapid onset of a second peak with a mass that corresponds to lyso-BCAT and/or BCAT-acetal ( $m/z$  469). This peak reached its maximum area at ~120 min, then slowly decreased to less than 20% after 24 h. Hydrolysis of BCAT at pH 4.5 followed a slower kinetic response, with approximately 30% cleavage occurring within 200 min. The time-dependent  $^1\text{H-NMR}$  analysis of BCAT hydrolysis is shown in Fig. 2C. Very rapid loss of the vinyl ether  $\alpha$ -proton peaks (~6.0 ppm) and concomitant onset of an aldehyde peak at 9.7 ppm was observed within 5 min. Inte-

gration of the aldehyde peak indicated >90% aldehyde product formation after 10 min. A doublet at 4.8 ppm corresponding to the BCAT-acetal ring proton was also observed, although it appears to be only a very minor component (<5%, data not shown). Taken together, these studies suggest that BCAT hydrolysis does not involve significant formation of BCAT-acetal, but proceeds instead to the fully hydrolyzed materials, 1-octadecenal and *O*-(1-glyceryl)-*N*-(bis-2-aminoethyl)-carbamate (GCAT).

#### Transfection Complex Formation

BCAT and DCAT transfection complexes were formed by adding the lipids to plasmid DNA in an isotonic 40% ethanol/dextrose solution, followed by removal of the ethanol under vacuum. The final DNA concentration was 0.6 mg/ml, with lipid:DNA charge ratios of 2:1, 4:1, or 6:1. Dynamic light

scattering analysis of the transfection complexes yielded an average diameter range between 300–400 nm, with a polydispersity value indicative of a heterogeneous size distribution. Polydispersity was also observed during freeze fracture electron microscopy analysis of the 4:1 BCAT:DNA complexes shown in Fig. 3. The majority of particles ranged between 50 and 300 nm (Fig. 3A); however, some aggregates approached 1  $\mu\text{m}$  in diameter (Fig. 3B). The smaller particles were spherical, multilamellar structures. No evidence of nonspherical structures was apparent (42).

### Optimization of Formulation and Transfection

The transfection efficiency of BCAT and DCAT were optimized for lipid:DNA charge ratio and helper lipid molar ratio by monitoring transgene expression of luciferase activity in NIH-3T3 cells. These experiments were performed under two DNA dose regimes (0.2  $\mu\text{g}/\text{well}$  and 1.0  $\mu\text{g}/\text{well}$ ). Studies were also conducted in the presence and absence of 10% serum in the medium. Both BCAT (Fig. 4A) and DCAT (Fig. 4B) exhibited optimum levels of activity at  $\geq 4:1$  +/- charge ratios. For both formulations, the difference between the 0.2  $\mu\text{g}$  dose and the 1.0  $\mu\text{g}$  dose diminished at a 4:1 charge ratio. Serum was found to enhance transfection by a factor of 5–10 at all charge ratios examined. The observed luciferase activi-

ties was also typically five- to tenfold higher for the acid-labile BCAT formulations compared with the nonlabile DCAT complexes. At a 4:1 +/- charge ratio, both BCAT and DCAT exhibited two to three orders of magnitude higher levels of expression compared with an optimized DOTMA:Chol formulation. While maintaining the optimal 4:1 +/- charge ratio, the effect of DOPE on luciferase activity was also probed (Fig. 5). A slight enhancement in activity was observed in BCAT and DCAT formulations containing 20 mol% DOPE. Further increase in the DOPE molar ratio led to decreased transgene activity. Because the effect of DOPE on expression levels was found to be small, it was omitted in all subsequent transfection experiments. It was also noted that no significant loss in transfection activity was observed for BCAT and DCAT transfection complexes stored at 4°C for 1 week, whereas similar treatment of DOTMA:Chol formulations resulted in a 40% decrease in activity.

Lipid toxicity was also probed by incubating NIH-3T3 cells for 24 h in the presence of BCAT, DCAT, and DOTMA:Chol transfection complexes. Visual observation of the cells treated with 4:1 BCAT:DNA revealed normal cell proliferation and morphology with no obvious signs of toxicity. The cells treated with DCAT exhibited reduced proliferation with >50% cells showing a contracted morphology. Likewise, cells treated with DOTMA:Chol exhibited reduced

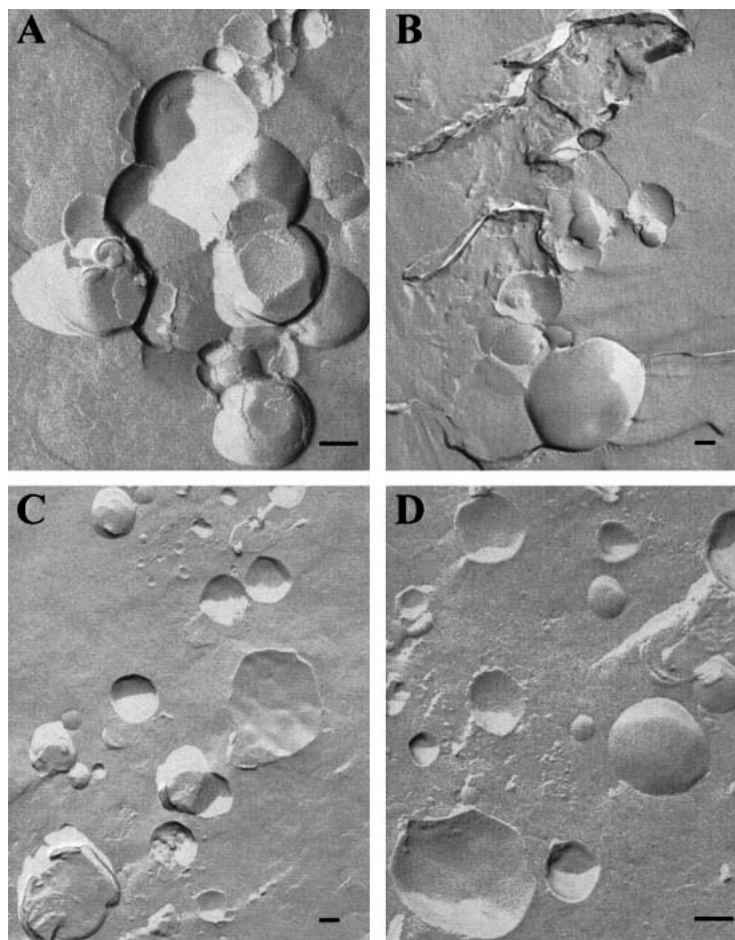


**Fig. 3.** Freeze fracture electron microscopy of 4:1 BCAT:DNA complexes. Bars represent 100 nm. (A, B) Examples of the large aggregates formed. (C, D) Representative population of monomeric particles and small aggregates.

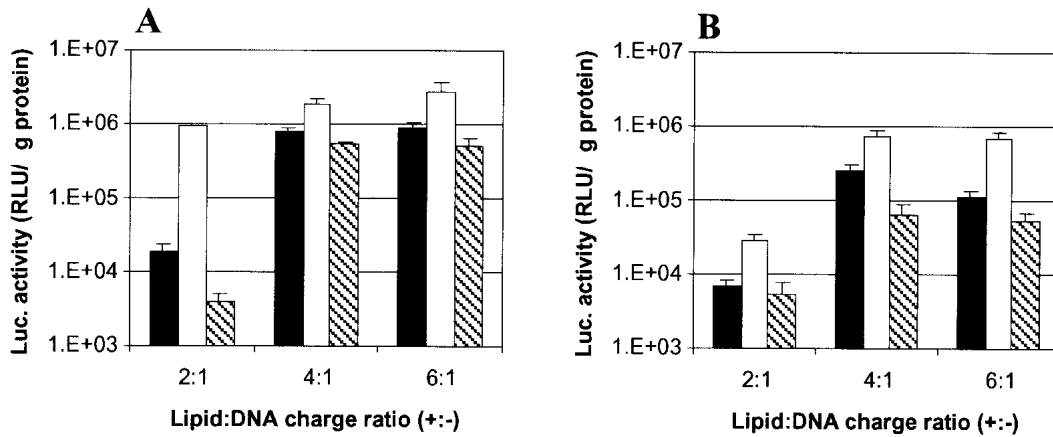


**Fig. 4.** Optimization of complex formation and transfection conditions in NIH-3T3 cells followed by expressed luciferase activity in the presence and absence of 10% serum. (A) BCAT: ■ 0.2 µg DNA/well, + 10% serum; □ 1.0 µg DNA/well, + 10% serum; ▨ 1.0 µg DNA/well without serum. (B) DCAT: ■ 0.2 µg DNA/well, + 10% serum; □ 1.0 µg DNA/well, + 10% serum; ▨ 1.0 µg DNA/well without serum. The observed luciferase expression levels for DOTMA:Chol in the absence of serum were  $1116 \pm 126$  at 0.2 µg/well DNA loading and  $2031 \pm 278$  at 1 µg/well DNA loading. Control cells exhibited background luminescence of  $49.3 \pm 0.6$ . Expression levels are reported as mean activity  $\pm$  standard deviation ( $n=4$ ).

proliferation; significant cell death (25–50%) was also observed, with all remaining cells in a contracted morphologic state.

#### Transfection in Multiple Cell Lines

We compared transfection levels for optimized formulations in four cell lines: NIH-3T3, SCCVII, RENCA, and HUVEC (Fig. 6). BCAT exhibited similar luciferase activity in all four cell lines, with expression levels that averaged five to eight times greater than those observed for DCAT. BCAT expression levels were two to three orders of magnitude higher than for optimized DOTMA:Chol formulations in all cell lines except HUVEC.

#### Transfection Complex Uptake and Expression

Experiments designed to detect different levels of transgene uptake and expression were then performed using fluo-

rescence assisted cell sorting (FACS) to monitor the relative efficiencies of BCAT, DCAT, and DOTMA:Chol formulations. A psoralen-labeled plasmid was used to track uptake levels and a plasmid encoding green fluorescence protein (GFP) was used as an indicator of expression levels (Fig. 7). After a 4-h exposure of NIH-3T3 cells to the transfection complexes, FACS analysis showed that DOTMA:Chol formulations were 2.5 times more effective in promoting plasmid uptake than BCAT and 4 times more efficient than DCAT. In spite of their lower uptake levels, BCAT transfection complexes promoted 1000 times more GFP expression than DOTMA:Chol, whereas DCAT was 360-fold more effective than DOTMA:Chol (i.e., 1000:360:1 relative efficiency based on GFP expression). In each formulation, greater than 95% of all cells were positive for plasmid uptake; however, both BCAT (50%) and DCAT (32%) showed significantly higher percentages of GFP-expressing cells than DOTMA:Chol

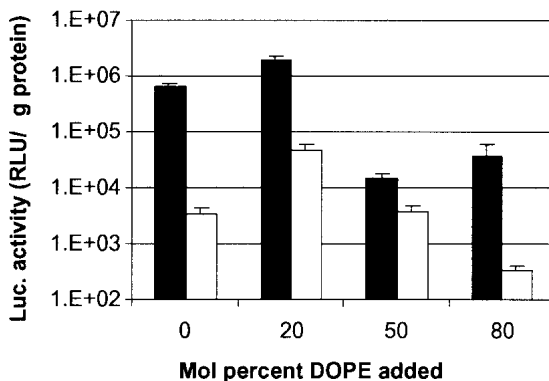


**Fig. 5.** Effect of helper lipid (DOPE) on the transfection efficiency of BCAT and DCAT monitored by luciferase activity in NIH-3T3 cells (4:1 +/- charge ratio; 1.0 µg/well DNA). Expression levels are shown for BCAT:DOPE (■) and DCAT:DOPE (□) at molar ratios of 100:0, 80:20, 50:50, 20:80. The observed luciferase activity for DOTMA:Chol was  $2031 \pm 278$  at 1 µg/well DNA loading. Control cells exhibited background luminescence of  $179.9 \pm 41.1$ . Expression levels are reported as mean activity  $\pm$  standard deviation ( $n=4$ ).

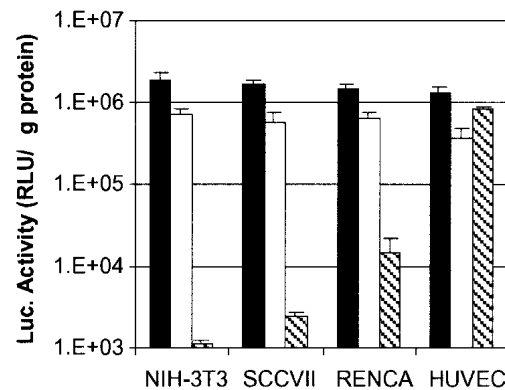


**Fig. 6.** Comparison of luciferase activity across multiple cell lines for BCAT (■) and DCAT (□). Cells were transfected with 1.0 µg of DNA added per well with a lipid:DNA charge ratio of 4:1. Control cells exhibited background luminescence of  $49 \pm 0.6$ ,  $52 \pm 8.0$ ,  $40 \pm 10$ , and  $286 \pm 127$  for NIH-3T3, SCCVII, RENCA, and HUVEC cells, respectively. Expression levels are reported as mean activity  $\pm$  standard deviation ( $n=4$ ).

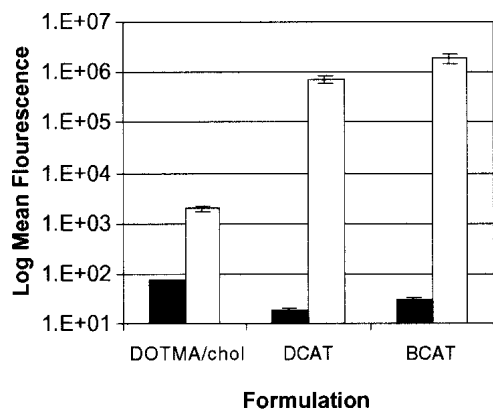


**Fig. 7.** DNA uptake vs. GFP expression in NIH-3T3 cells monitored by FACS analysis. ■ Uptake of psoralen-labeled DNA after 4 h incubation with transfection complexes and washing to remove unbound material. □ Expression of GFP 24 h after treatment with transfection complexes. In both cases the data are reported as log mean fluorescence of the population  $\pm$  standard deviation (average of two experiments).

(9%). Thus, the observed relative transfection efficiencies for BCAT, DCAT, and DOTMA:Chol on a per cell basis were 5.6:3.6:1, respectively.

#### *In Vivo* Transfection

A comparison of *in vivo* chloramphenicol acetyltransferase (CAT) expression levels in lung and subcutaneous SCC-VII tumor is shown in Fig. 8. C3H mice were administered a 90  $\mu$ g dose of DNA (0.3 mg/ml) via a tail vein administration of *in vitro*-optimized cationic lipid:CAT plasmid formulations (i.e., 4:1  $\pm$  charge ratio for BCAT and DCAT and 3:1 charge ratio for DOTMA:Chol). The lung and tumor tissues were harvested after 48 h and CAT expression characterized via enzyme-linked immunosorbent assay ELISA assay. DOTMA:Chol complexes produced 1000 times more expression in lung relative to tumor. In contrast, BCAT transfection complexes displayed only tenfold higher expression levels in lung, presumably due to reduced lung uptake levels, with identical

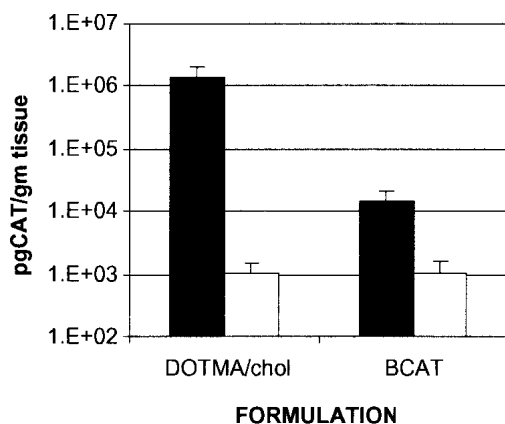


**Fig. 8.** *In vivo* gene transfer following IV administration of BCAT transfection complexes. BCAT and DOTMA:Chol based transfection complexes were formed with a CAT expression plasmid. A 90- $\mu$ g plasmid dose was administered via the tail vein in SCCVII tumor bearing C3H mice. Tissue was harvested 24 h after administration and analyzed for CAT expression in ■ lung and □ tumor.

expression levels in tumor compared with the DOTMA:Chol standard. It is important to note that the formulation characteristics were visibly different for BCAT and DCAT in these experiments. BCAT complexes were well tolerated and showed no indications of acute toxicity. All mice treated with DCAT formulations, however, died shortly after the treatment regime. Although no detailed toxicology was performed, the DOTMA complexes produced small, white, necrotic spots in the liver, whereas none were observed in the livers of animals treated with BCAT complexes. These observations suggest that DCAT and DOTMA have higher *in vivo* toxicities arising either from the lipids themselves or due to the biophysical properties of their complexes under systemically circulating conditions.

#### DISCUSSION

At present, most lipid-based gene therapy formulations are inefficient and acutely cytotoxic, making them impractical for many clinical applications. Because endosomal escape and transfection complex disassembly within the cell have been shown to be among the most significant barriers for successful transgene expression (28,29), we hypothesized that incorporation of an acid-labile vinyl ether linkage into the cationic lipid would improve the gene transfer efficiency by (i) facilitating endosomal escape, (ii) improving the rate of complex disassembly, and (iii) degrading the cationic lipid carrier to biocompatible components. The viability of this approach has been previously demonstrated with diplasmeylcholine vesicles that are stable at pH 7.4, but degraded within acidic endosomal compartments to promote efficient cytoplasmic delivery via endosomal membrane destabilization and/or fusion (38,39,43). If BCAT-based transfection complexes are also internalized via an endocytotic pathway, acid-catalyzed vinyl ether hydrolysis might promote endosomal escape via a similar mechanism. In addition, once separated from the lipid anchor, it is likely that the diethylenetriamine headgroup may be more accessible to cellular cation exchange, thereby improving the bioavailability of the transgene.

BCAT and DCAT both formed transfection complexes that were physically stable and retained >90% of their activity for at least 1 week. Although small particles were the predominant form in solution, the large aggregates observed in these samples may be the result of particle aggregation mediated by plasmid DNA condensation of multiple small particles to give multilamellar structures (44). In addition, transfection complexes formed from BCAT and DCAT exhibited (i) optimal transfection levels at a 4:1  $\pm$  charge ratio, (ii) improved transfection activity in the presence of 10% serum, and (iii) slightly improved transgene expression on incorporation of DOPE as helper lipid. Most notably, BCAT and DCAT transfection complexes produced consistently high levels of transfection across four different cell lines (NIH-3T3, SCCVII, RENCA, and HUVEC) relative to DOTMA:Chol controls.

At an optimized 4:1  $\pm$  charge ratio, BCAT formulations typically exhibited three orders of magnitude higher transgene expression than an optimized DOTMA:Chol formulation, despite a 2.5-fold less efficient cellular uptake activity. DCAT also showed inefficient uptake; however, the internalized complexes displayed 300-fold higher transgene activity than DOTMA:Chol complexes. Because BCAT typi-

cally showed only three- to fivefold higher levels of transgene activity and expression than DCAT, a common mechanism of action is suggested for both BCAT and DCAT transfection complexes. These observations generally support the design principle of degradative enhancement of transgene expression; however, they do not directly explain the surprisingly high levels of DCAT expression relative to BCAT. We infer from these results that competing complex dissociation pathways may be operating in addition to the acid-catalyzed dealkylation route engineered into the BCAT lipid vehicle. It is likely that the diethylenetriamine headgroup used in these experiments may be the primary structural element leading to increased transgene expression. This could arise from an intramolecular cationic headgroup cleavage reaction involving carbamate attack by a distal (free) amine to displace a cyclic urea fragment from the dialkylglycerol backbone (Fig. 9). It could also occur by involvement of the decomplexation/endosomal escape mechanism proposed by Szoka and co-workers (45,46). In the latter case, membrane-membrane contact between the transfection complex and the negatively charged target membrane induces anionic lipid flip-flop that facilitates displacement of DNA across cellular membrane barriers. The diethylenetriamine headgroup may be unusually active in promoting this mechanism for BCAT and DCAT transfection complex disassembly, leading to a substantial increase in transgene activity relative to DOTMA:Chol. If this premise is correct, then it is the concurrent BCAT acid hydrolysis mechanism that is responsible for the additional three- to fivefold increase in activity relative to DCAT. A third possibility is that both BCAT and DCAT transfection complexes escape the endosome via similar mechanisms, but that downstream cellular processing events (e.g., disassembly, intracellular transport, protease digestion, or nuclear localization/processing) proceed at different rates.

Toxicity is another key issue in many cationic lipid gene delivery formulations. Reduced toxicity has been achieved by incorporation of biologically cleavable linkages such as esters, amides, and carbamates (33). The serum stability and pharmacokinetics of these systems, however, may be adversely affected by degradation *in vivo* catalyzed by plasma factors during circulation. The use of a serum stable, disulfide linkage was shown to decrease *in vitro* toxicity relative to a nonreducible analog and DC-Chol controls (33). In our studies a relative toxicity order of BCAT < DCAT < DOTMA:Chol was observed. NIH-3T3 cells treated with 4:1 BCAT:DNA transfection complexes for 24 h exhibited normal proliferation and no morphologic changes, whereas cells treated with DCAT exhibited decreased proliferation and contracted morphology in more than 50% of the population. Cells treated with DOTMA:Chol showed reduced proliferation and 25–

50% cell death; all remaining cells displayed a contracted morphology. Taken together, these results suggest that the vinyl ether and carbamate cleavable linkages improve the biologic compliance of BCAT and DCAT *in vitro* relative to DOTMA:Chol.

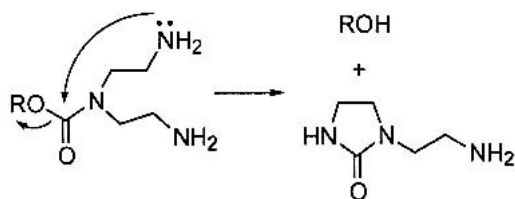
Preliminary *in vivo* experiments conducted with *in vitro*-optimized BCAT, DCAT, and DOTMA:Chol formulations showed that BCAT transfection complexes exhibited modest levels of CAT activity and no obvious signs of toxicity. Interestingly, BCAT transfection complexes showed less CAT expression in the lung relative to DOTMA:Chol, while maintaining similar expression levels in a subcutaneous SCCVII tumor and in the liver. Although full assessment of *in vivo* transfection activity would require more extensive dose-response and biodistribution studies, this initial analysis shows that, with the exception of lung, BCAT complex expression levels were higher in tumor than any other organ. The additional observation that all mice treated with DCAT died, whereas none of the mice treated with BCAT exhibited any obvious signs of toxicity, also suggests that the acute *in vivo* toxicity of BCAT is low. Thus, the choice of the diethylenetriamine headgroup in connection with acid-catalyzed separation of the cationic headgroup from the hydrophobic anchor appears to significantly reduce the toxicity of BCAT transfection complexes. These results further suggest that BCAT may be a viable *in vivo* transfection agent, especially with formulation modifications such as the incorporation of polyethylene glycol and targeting agents to further enhance their specificity for delivery of toxic genes to tumor cells.

In summary, the incorporation of acid-labile linkages in cationic lipids bearing diethylenetriamine headgroups leads to significantly increased transgene activity and reduced toxicity relative to a commonly used, optimized DOTMA:Chol formulation. The acid-labile linkages of BCAT generated smaller increases in transgene activity relative to DCAT than expected, suggesting that the hydrolysis/disassembly mechanism may be slow relative to endosomal escape and processing promoted by the diethylenetriamine headgroup. A more acid-labile linkage would, therefore, be expected to speed up the cleavage reaction. Current efforts are directed toward examining this hypothesis.

## EXPERIMENTAL

### Synthesis of BCAT and DCAT

2,2'-Dipyridyl carbonate was purchased from TCI America (Portland, Oregon). DOPE was obtained from Avanti Polar Lipids (Alabaster, Alabama). All other compounds were purchased from Aldrich (Milwaukee, Wisconsin) and used without further purification unless otherwise stated. Triethylamine and diisopropylamine were distilled from CaH<sub>2</sub>. Spectrophotometric grade solvents were dried over an appropriate desiccant and then distilled before use. All reactions were performed under an argon atmosphere. BCAT was synthesized as previously described (40). DCAT was synthesized in five steps from 3-*O*-(*t*-butyldiphenylsilyl)-*rac*-glycerol as outlined in Fig. 1. The purities of BCAT and DCAT (>98%) were established by NMR, MS, and TLC. Lipids were stored frozen as benzene solutions until needed to prevent the acid-catalyzed degradation that can occur with extended storage of chloroform solutions. After 10 months,



R = dialkyl- or dialkenyl- glyceryl

Fig. 9.

NMR analysis indicated that no significant degradation occurred in benzene stock solutions that were stored under these conditions.

***O*-(1,2-Di-*O*-(9'*Z*-octadecyl)-glycerol)-*N*-(bis-2-phthalamidylethyl)-carbamate (4)**

1,2-Di-*O*-(9'*Z*-octadecyl)-*rac*-glycerol (2, 516 mg, 0.87 mmol), 2,2'-dipyridyl carbonate (282 mg, 1.3 mmol) and triethylamine (1.8 ml, 12.9 mmol) were stirred for 2 days in 20 ml CH<sub>2</sub>Cl<sub>2</sub> before extracting the reaction mixture with 5% NaHCO<sub>3</sub> (75 ml) and saturated brine (75 ml). The CH<sub>2</sub>Cl<sub>2</sub> layer was dried over Na<sub>2</sub>SO<sub>4</sub>, filtered, and evaporated. The resulting oil was redissolved in CH<sub>2</sub>Cl<sub>2</sub> (20 ml), 1,5-diphthalamidyl diethylenetriamine (337 mg, 0.93 mmol) added and the reaction stirred for 2 days. The solution was evaporated and the crude mixture purified via flash chromatography (3:2 hexane: ether), yielding 592 mg of a pale yellow oil (69% yield). TLC (1:2 hexane: ether, UV, acidic molybdate/heat): R<sub>f</sub> = 0.33. <sup>1</sup>H-NMR (C<sub>6</sub>D<sub>6</sub>): 0.89 (t, *J* = 6 Hz, 6H), 1.1–1.45 (m, 44H), 1.45–1.67 (m, 4H), 2.07 (m, 8H), 3.32–3.75 (m, 15H), 4.02 (m, 2H), 5.48 (m, 4H), 6.92 (m, 4H), 7.47 (m, 4H). <sup>13</sup>C-NMR (C<sub>6</sub>D<sub>6</sub>): 14.3 (O), 23.1 (E), 26.6 (E), 27.7 (E), 29.6–30.2 (E), 32.3 (E), 33.1 (E), 36.0 (E), 45.4 (E), 46.2 (E), 65.2 (E), 70.6 (E), 71.3 (E), 71.7 (E), 77.3 (O), 123.0 (O), 130.1 (O), 130.2 (O), 132.5 (E), 132.7 (E), 133.3 (O), 133.5 (O), 156.0 (E), 167.7 (E), 168.0 (E).

***O*-(1,2-Di-*O*-(9'*Z*-octadecyl)-glycerol)-*N*-(bis-2-aminoethyl)-carbamate (6)**

*O*-(1,2-*O*-Diioleyl-*rac*-glycerol)-*N*-(di-2-phthalamidylaminoethyl)-carbamate (4, 160 mg, 0.16 mmol) was dissolved in 60 ml methanol before the addition of hydrazine hydrate (1.0 ml, 21 mmol). The reaction was stirred for 1 day, then evaporated to dryness, yielding an off-white precipitate. Chloroform (50 μl) was added and the insoluble side product removed via filtration. The filtrate was evaporated and dried *in vacuo* overnight, yielding 116 mg of a pale yellow oil (99% yield). TLC (80:19.5:0.5 CHCl<sub>3</sub>:MeOH:NH<sub>4</sub>OH, UV, acidic molybdate/heat): R<sub>f</sub> = 0.80. <sup>1</sup>H-NMR (C<sub>6</sub>D<sub>6</sub>): 0.89 (t, 6H), 1.1–1.45 (m, 44H), 1.45–1.65 (m, 4H), 1.9–2.2 (m, 8H), 2.63 (t, *J* = 6 Hz, 4H), 3.00–3.80 (m, 11H), 4.26 (dd, *J*<sub>1</sub> = 9 Hz, *J*<sub>2</sub> = 5 Hz, 1H) 4.47 (dd, *J*<sub>1</sub> = 10 Hz, *J*<sub>2</sub> = 5 Hz, 1H) 5.48 (m, 4H), <sup>13</sup>C-NMR (C<sub>6</sub>D<sub>6</sub>): 14.3 (O), 23.1 (E), 26.6 (E), 27.7 (E), 29.6–30.2 (E), 32.3 (E), 33.1 (E), 35.5 (E), 41.0 (E), 41.3 (E), 51.1 (E), 51.3 (E), 65.0 (E), 70.5 (E), 71.1 (E), 71.8 (E), 77.5 (O), 130.2 (O), 130.7 (O), 156.7 (E).

**BCAT Hydrolysis**

The hydrolysis of BCAT was monitored via 200 MHz <sup>1</sup>H-NMR. BCAT (4 mg) was dissolved in CD<sub>3</sub>CN (500 μl) and its spectrum recorded. Then, 50 μl of 2% or 0.2% DCl in D<sub>2</sub>O was added, the sample maintained at room temperature for the duration of the experiment, and NMR spectra recorded at various time points.

BCAT hydrolysis was also monitored via RP-HPLC. In this case, 4 mg of BCAT was dissolved in 1 ml methanol and 200 μl removed for the time zero measurement. Then 320 μl of 1 N or 0.1 N HCl was added and the mixture stirred at 37°C for the duration of the experiment. At each time point a 280 μl aliquot was removed; the sample was then neutralized with

80 μl 1N NaOH and extracted with 200 μl chloroform. The chloroform layer was evaporated under N<sub>2</sub> flow and redissolved in 50 μl fresh, deacidified chloroform. The samples were then injected onto a Waters Spherisorb® 4.6 × 150, 5 μm octadecasilane column (Milford, Massachusetts) using an isocratic 80:20 methanol:methylene chloride mobile phase and a SEDEX 55 evaporative light scattering detector (Sedere, Alfortville, France). The expected aldehyde product was observed primarily as its hydrated form, based on synthetic reference standards. Unfortunately, this equilibrium produced inconsistencies with the aldehyde-aldehyde hydrate extraction making it difficult to accurately quantify both the production of aldehyde as well as the disappearance of BCAT via this procedure.

**Preparation of Transfection Complexes**

DNA stock solutions (1.2 mg/ml) were prepared in 40% absolute ethanol containing 250 mM glucose, 25 mM NaCl, at pH 6 (adjusted with dilute acetic acid). Lipid stock solutions for transfection complex formation were prepared by dissolving a thin lipid film in 40% absolute ethanol containing 250 mM glucose, 25 mM NaCl, pH 6 at lipid concentrations that depended on the desired lipid:DNA ratio. The pH of these solutions was then adjusted to 6 using acetic acid. Complexes with 2:1, 4:1, and 6:1 lipid:DNA charge ratios and final DNA concentrations of 0.6 mg/ml were prepared by slowly adding the appropriate amount of DNA stock to an equivalent volume of lipid stock. The solutions were carefully evaporated and then placed under vacuum overnight to remove traces of ethanol. The samples were then rehydrated to the same final concentration using sterile H<sub>2</sub>O.

DOTMA:Chol formulations were prepared as described previously (47). After preparation of the DNA stock solution (600 μg/ml, 10% lactose) and the lipid stock solution (4:1 DOTMA:Cholesterol, 11.59 mM in DOTMA, 10% lactose), the desired amount of DNA stock was then slowly added to an equal volume of lipid stock with mild vortexing, yielding a final DNA concentration of 300 μg/ml at an optimized 3:1 +/- charge ratio.

**Freeze Fracture Electron Microscopy**

A 100-μl sample of 4:1 BCAT:DNA complex was prepared as described above. Glycerol was added to the sample for cryoprotection (final glycerol concentration <20% v/v). Approximately 10 μl of this solution was placed on a copper sample holder and then rapidly cooled by immersion into liquid ethane. The frozen samples were transferred to a Balzers 400T (Furstenstum, Lichtenstein) freeze fracture apparatus maintained at -120°C. The samples were then fractured and sputtered at a 45° angle with platinum, followed by carbon deposition at a 90° angle. The organic material was then digested overnight with bleach and the replicas observed with a Phillips CM 12 microscope (Hillsboro, Oregon) operating at 60 kV.

**In Vitro Transfection**

Twenty-four well plates were seeded with NIH-3T3, RENCA, SCCIV, or HUVEC cells at densities of 6 × 10<sup>4</sup> cells/well and then incubated in cell appropriate media for 24 h at 37°C and 5% CO<sub>2</sub>. The media was then carefully re-



moved, replaced with 1 ml of media containing transfection complexes (1 or 0.2  $\mu\text{g}/\text{ml}$  DNA) and the cells incubated for 4 h. The transfection media was then carefully removed, washed with phosphate buffered saline, replaced with fresh media, and reincubated for an additional 24 h prior to analysis.

#### Luciferase Assay

The media was removed and the cells washed two times with 1 ml phosphate buffered saline (PBS, -Mg, -Ca). Lysis buffer (500  $\mu\text{l}$ , Promega E4030, Madison, Wisconsin) was added and the cells were stored at  $-80^\circ\text{C}$  overnight. After thawing, cell lysates were removed from the wells via pipette and transferred to 1.5 ml microcentrifuge tubes. The tubes were centrifuged for 5 min at 9000 rpm, and 20  $\mu\text{l}$  of each supernatant was removed and placed in an opaque 96-well plate. Luminescence was monitored for 30 s/well following the addition of luciferase assay reagent (100  $\mu\text{l}$ , Promega E4030) using a luminometer. The luminescence intensity was then corrected by normalizing for total cellular protein content as determined via a modified Lowry assay.

#### Total Protein Assay

Total protein in cell lysate supernatant solutions was monitored utilizing the BIO-RAD detergent compatible protein assay (500-0112, Hercules, California) and bovine serum albumin (BSA) standards. Reagent solution (200  $\mu\text{l}$ ) and 5  $\mu\text{l}$  of standard or sample solution were combined in a 96-well plate, gently shaken for 10 min, then incubated at  $37^\circ\text{C}$  for 1 h. Absorbance was measured using a plate reader and converted to protein concentrations using a standard curve.

#### Fluorescence Activated Cell Sorting

##### Uptake

BCAT, DCAT, and DOTMA:Chol transfection complexes were prepared at optimal 4:1, 4:1, and 3:1 +/- charge ratios, respectively, with a psoralen labeled plasmid. NIH-3T3 cells were seeded at  $6 \times 10^4$  cells/well 24 h prior to treatment with complexes. The media was removed and replaced with 1 ml transfection media (1  $\mu\text{g}/\text{ml}$  DNA) and the cells were incubated for an additional 4 h. The cells were then washed two times with PBS (-Mg, -Ca), trypsinized, transferred to centrifuge tubes with PBS, and centrifuged. The supernatant was removed and the cells resuspended in PBS before FACS analysis. Uptake was measured by gating for cells positive for psoralen fluorescence.

##### Expression

BCAT, DCAT, and DOTMA:Chol transfection complexes were prepared at optimal 4:1, 4:1, and 3:1 +/- charge ratios, respectively, with a psoralen labeled plasmid. NIH-3T3 cells were seeded at  $6 \times 10^4$  cells/well 24 h prior to treatment with complexes. The media was removed and replaced with 1 ml transfection media (1  $\mu\text{g}/\text{ml}$  DNA) and the cells were incubated for an additional 4 h. The transfection media was replaced with fresh media and the cells incubated for 24 h. The cells were then washed two times with PBS (-Mg, -Ca), trypsinized, transferred to centrifuge tubes with PBS, and

centrifuged. The supernatant was removed and the cells resuspended in PBS before FACS analysis.

#### In Vivo Transfection

BCAT, DCAT, and DOTMA:Chol transfection complexes were prepared at optimal 4:1, 4:1, and 3:1 +/- charge ratios, respectively, with a CAT expression plasmid (47). Ten days after subcutaneous implantation of SCCVII tumor cells, C3H mice were administered a 90  $\mu\text{g}$  dose of DNA via tail vein injection. Forty-eight hours after administration, lung and tumor were harvested and analyzed for CAT expression via ELISA assay.

#### ACKNOWLEDGMENTS

The authors wish to thank the NIH GM55266 and Valentis, Inc. for financial support. All plasmids used in these studies were a gift of Valentis, Inc. The expertise of Dr. H. Dorota Inerowicz (HPLC) and Cathy Wolken (Ohio State University, freeze fracture electron microscopy) is also gratefully acknowledged.

#### REFERENCES

1. M. S. Horwitz. *Adenoviridae and Their Replication*. Raven Press, New York, 1990.
2. A. P. Rolland. From genes to gene medicines: recent advances in nonviral gene delivery. *Crit. Rev. Ther. Drug Carrier Sys.* **15**:143-198 (1998).
3. K. Anwer, A. Bailey, and S. M. Sullivan. Targeted gene delivery: a two-pronged approach. *Crit. Rev. Ther. Drug Carrier Sys.* **17**:377-424 (2000).
4. A. D. Miller. Human gene-therapy comes of age. *Nature* **357**:455-460 (1992).
5. A. V. Kabanov and V. A. Kabanov. DNA complexes with poly-cations for the delivery of genetic material into cells. *Bioconj. Chem.* **6**:7-20 (1995).
6. M. Ibanez, P. Gariglio, P. Chavez, R. Santiago, C. Wong, and I. Baeza. Spermidine condensed DNA and cone-shaped lipids improve delivery and expression of exogenous DNA transfer by liposomes. *Biochem. Cell Biol.* **74**:633-643 (1996).
7. S. Ferrari, A. Pettenazzo, N. Garbati, F. Zacchello, J. P. Behr, and M. Scarpa. Polyethylenimine shows properties of interest for cystic fibrosis gene therapy. *Biochim. Biophys. Acta* **1447**:219-225 (1999).
8. P. Erbacher, J. S. Remy, and J. P. Behr. Gene transfer with synthetic virus-like particles via the integrin-mediated endocytosis pathway. *Gene Ther.* **6**:138-145 (1999).
9. B. Abdallah, A. Hassan, C. Benoist, D. Goula, J. P. Behr, and B. A. Demeneix. A powerful nonviral vector for in vivo gene transfer into the adult mammalian brain: polyethylenimine. *Human Gene Ther.* **7**:1947-1954 (1996).
10. S. Vinogradov, E. Batrakova, S. Li, and A. Kabanov. Polyion complex micelles with protein-modified corona for receptor-mediated delivery of oligonucleotides into cells. *Bioconj. Chem.* **10**:851-860 (1999).
11. T. K. Bronich, H. K. Nguyen, A. Eisenberg, and A. V. Kabanov. Recognition of DNA topology in reactions between plasmid DNA and cationic copolymers. *J. Am. Chem. Soc.* **122**:8339-8343 (2000).
12. H.-K. Nguyen, P. Lemieux, S. V. Vinogradov, C. L. Gebhart, N. Guerin, G. Paradis, T. K. Bronich, V. Y. Alakhov, and A. V. Kabanov. Evaluation of polyether-polyethylenimine graft copolymers as gene transfer agents. *Gene Ther.* **7**:126-138 (2000).
13. E. Wagner, M. Cotten, R. Foisner, and M. L. Birnstiel. Transferin polycation DNA complexes—the effect of polycations on the structure of the complex and DNA delivery to cells. *Proc. Natl. Acad. Sci. USA* **88**:4255-4259 (1991).
14. G. Y. Wu and C. H. Wu. Evidence for targeted gene delivery to Hep G2 hepatoma-cells *in vitro*. *Biochemistry* **27**:887-892 (1988).

15. S. Li, M. A. Rizzo, S. Bhattacharya, and L. Huang. Characterization of cationic lipid-protamine-DNA (LPD) complexes for intravenous gene delivery. *Gene Ther.* **5**:930-937 (1998).
16. F. L. Sorgi, S. Bhattacharya, and L. Huang. Protamine sulfate enhances lipid-mediated gene transfer. *Gene Ther.* **4**:961-968 (1997).
17. O. Zelphati, X. W. Liang, P. Hobart, and P. L. Felgner. Gene chemistry: functionally and conformationally intact fluorescent plasmid DNA. *Human Gene Ther.* **10**:15-24 (1999).
18. D. Singh, S. K. Bisland, K. Kawamura, and J. Garipey. Peptide-based intracellular shuttle able to facilitate gene transfer in mammalian cells. *Bioconj. Chem.* **10**:745-754 (1999).
19. C. Ben Mamoun, R. Truong, I. Gluzman, N. S. Akopyants, A. Oksman, and D. E. Goldberg. Transfer of genes into *Plasmodium falciparum* by polyamidoamine dendrimers. *Mol. Biochem. Parasitol.* **103**:117-121 (1999).
20. T. Hudde, S. A. Rayner, R. M. Comer, M. Weber, J. D. Isaacs, H. Waldmann, D. P. F. Larkin, and A. J. T. George. Activated polyamidoamine dendrimers, a non-viral vector for gene transfer to the corneal endothelium. *Gene Ther.* **6**:939-943 (1999).
21. A. D. Miller. Cationic liposomes for gene therapy. *Angew. Chem., Int. Ed.* **37**:1769-1785 (1998).
22. A. Chonn and P. R. Cullis. Recent advances in liposome technologies and their applications for systemic gene delivery. *Adv. Drug Delivery Rev.* **30**:73-83 (1998).
23. K. W. C. Mok, A. M. I. Lam, and P. R. Collis. Stabilized plasmid-lipid particles: factors influencing plasmid entrapment and transfection properties. *Biochim. Biophys. Acta* **1419**:137-150 (1999).
24. G. Byk, C. Dubertret, V. Escriou, M. Frederic, G. Jaslin, R. Rangara, B. Pitard, J. Crouzet, P. Wils, B. Schwartz, and D. Scherman. Synthesis, activity, and structure-activity relationship studies of novel cationic lipids for DNA transfer. *J. Med. Chem.* **41**:224-235 (1998).
25. R. G. Cooper, C. J. Etheridge, L. Stewart, J. Marshall, S. Rudginsky, S. H. Cheng, and A. D. Miller. Polyamine analogues of 3  $\beta$ -[N-(N',N'-dimethylaminoethane)carbomoyl]cholesterol (DC-Chol) as agents for gene delivery. *Chem. Eur. J.* **4**:137-151 (1998).
26. J. S. Remy, C. Sirlin, P. Vierling, and J. P. Behr. Gene-transfer with a series of lipophilic DNA-binding molecules. *Bioconj. Chem.* **5**:647-654 (1994).
27. J. H. Felgner, R. Kumar, C. N. Sridhar, C. J. Wheeler, Y. J. Tsai, R. Border, P. Ramsey, M. Martin, and P. L. Felgner. Enhanced gene delivery and mechanism studies with a novel series of cationic lipid formulations. *J. Bio. Chem.* **269**:2550-2561 (1994).
28. M. B. Bally, P. Harvie, F. M. P. Wong, S. Kong, E. K. Wasan, and D. L. Reimer. Biologic barriers to cellular delivery of lipid-based DNA carriers. *Adv. Drug Del. Rev.* **38**:291-315 (1999).
29. J. Zabner, A. J. Fasbender, T. Moninger, K. A. Poellinger, and M. J. Welsh. Cellular and molecular barriers to gene transfer by a cationic lipid. *J. Bio. Chem.* **270**:18977-19007 (1995).
30. S. C. Davis and F. C. Szoka. Conditionally stable liposomes for gene delivery. *ACS Symp. Ser.* **728**:179-189 (1999).
31. C. C. Pak, S. Ali, A. S. Janoff, and P. Meers. Triggerable liposomal fusion by enzyme cleavage of a novel peptide-lipid conjugate. *Biochim. Biophys. Acta* **1372**:13-27 (1998).
32. F. Tang and J. A. Hughes. Introduction of a disulfide bond into a cationic lipid enhances transgene expression of plasmid DNA. *Biochem. Biophys. Res. Comm* **242**:141-145 (1998).
33. F. Tang and J. A. Hughes. Use of dithioglycolic acid as a tether for cationic lipids decreases the cytotoxicity and increases transgene expression of plasmid DNA *in vitro*. *Bioconj. Chem.* **10**:791-796 (1999).
34. F. Tang, W. Wang, and J. A. Hughes. Cationic liposomes containing disulfide bonds in delivery of plasmid DNA. *J. Liposome Res.* **9**:331-347 (1999).
35. A. M. Aberle, F. Tablin, J. Zhu, N. J. Walker, D. C. Gruenert, and M. H. Nantz. A novel tetraester construct that reduces cationic lipid-associated cytotoxicity. Implications for the onset of cytotoxicity. *Biochemistry* **37**:6533-6540 (1998).
36. S. Obika, W. Yu, A. Shimoyama, T. Uneda, T. Minami, K. Miyashita, T. Doi, and T. Imanishi. Properties of cationic liposomes composed of cationic lipid YKS-220 having an ester linkage: adequate stability, high transfection efficiency, and low cytotoxicity. *Bio. Pharm. Bull.* **22**:187-190 (1999).
37. J. Y. Legendre and F. C. Szoka. Delivery of plasmid DNA into mammalian-cell lines using pH-sensitive liposomes—comparison with cationic liposomes. *Pharm. Res.* **9**:1235-1242 (1992).
38. Y. Rui, S. Wang, P. S. Low, and D. H. Thompson. Diplasmenylcholine-folate liposomes: an efficient vehicle for intracellular drug delivery. *J. Am. Chem. Soc.* **120**:11213-11218 (1998).
39. M. M. Qualls and D. H. Thompson. Synergistic phototoxicity of chloroaluminum phthalocyanine tetrasulfonate delivered via acid-labile diplasmenylcholine-folate liposomes. *Int. J. Cancer* **93**:384-392 (2001).
40. J. A. Boomer and D. H. Thompson. Synthesis of acid-labile diplasmenyl lipids for drug and gene delivery applications. *Chem. Phys. Lipids* **99**:145-153 (1999).
41. J. R. Keefe and A. J. Kresge. Chapter title. In Z. Rappoport (ed.), *The Chemistry of Enols*. Wiley, Chichester, NY, 1990. pp. 399-480.
42. B. Sternberg, F. L. Sorgi, and L. Huang. New structures in complex-formation between DNA and cationic liposomes visualized by freeze-fracture electron-microscopy. *FEBS Lett.* **356**:361-366 (1994).
43. O. V. Gerasimov, A. Schwan, and D. H. Thompson. Acid-catalyzed plasmenylcholine hydrolysis and its effect on bilayer permeability: a quantitative study. *Biochim. Biophys. Acta* **1324**:200-214 (1997).
44. J. O. Radler, I. Koltover, T. Salditt, and C. R. Safinya. Structure of DNA-cationic liposome complexes: DNA intercalation in multilamellar membranes in distinct interhelical packing regimes. *Science* **275**:810-814 (1997).
45. O. Zelphati and F. C. Szoka. Mechanism of oligonucleotide release from cationic liposomes. *Proc. Natl. Acad. Sci. USA* **93**:11493-11498 (1996).
46. Y. H. Xu and F. C. Szoka. Mechanism of DNA release from cationic liposome/DNA complexes used in cell transfection. *Biochemistry* **35**:5616-5623 (1996).
47. K. Anwer, C. Meaney, G. Kao, R. Shelvin, R. M. Earls, P. Leonard, A. P. Rolland, and S. M. Sullivan. *J. Drug Target.* **8**:125-135 (2000).